ciable. The behavior of n_s mirrors the temperature dependence of the gap anisotropy. The nonzero values of n_s near T_c are consistent with those of Dessau *et al.* (*5*) and, we speculate, may be due to superconducting fluctuations.

As an additional check, we fabricated samples with different oxygen and cation stoichiometries. Different samples exhibited the same size gap at low temperatures, one in the Γ-M̄ and another in the Γ-X direction. We found a growing gap anisotropy with increasing temperature, the same behavior as in Fig. 4A.

We also checked the effect of the normal state (quasi-particle) binding energy. We compared samples where the quasi-particle binding energy along the Γ-M̄ direction of one sample and that along the Γ-X direction of a different sample were the same. The difference illustrated in Fig. 4 persisted. We conclude that the difference is related to the two symmetry directions, rather than the absolute size of the superconducting gap or the quasi-particle binding energy from which the photoemission superconducting condensate arises.

Because quantitative calculations comparing to our experimental data of Figs. 2 through 4 are not currently available, we neither endorse nor rule out specific models (*8*, *9*, *11*–*15*). Instead, we note how various models are constrained by our results. Any model must explain how the gap anisotropy arises. More stringent is that any model must explain how the anisotropy changes from 1.8:1 at $0.40T_c$ to at least 14:1 at $0.85T_c$, a change of a factor of 8 or 9. The increasing gap anisotropy as the temperature approaches T_c is a peculiar feature of high-temperature superconductors. A conventional BCS superconductor such as lead can have a gap anisotropy at low temperatures (*6*); however, this anisotropy disappears as T_c is approached from below (*6*).

Our data can be interpreted in terms of a two-component order parameter (*6*), of which there are several models (*13*, *16*). One possibility is a model that exhibits only a $d_{x^2-y^2}$ symmetry component near T_c and both components at lower temperatures. It is noteworthy that the best fit to our data at 70 K and above along the Γ-X direction yields a zero gap (*8*, *9*).

However, such two-component models (*13*, *16*) do not yet provide a quantitative analysis of the temperature dependence of the two components. Earlier theoretical work on the superconducting order parameter symmetry (*14*) indicates that two transition temperatures should be observed for a two-component order parameter. We note a recent, unpublished mean field analysis of a two-component order parameter (*15*); the investigators assumed an order parameter that is a mixture of *s*- and *d*-wave components. Minimization of the corresponding Ginzburg-Landau free energy gives a temperature-dependent gap anisotropy.

REFERENCES AND NOTES

1. C. G. Olson *et al.*, *Science* **245**, 731 (1989).
2. Z.-X. Shen *et al.*, *Phys. Rev. Lett.* **70**, 1553 (1993).
3. Y. Hwu *et al.*, *ibid.* **67**, 2573 (1991).
4. R. J. Kelley, J. Ma, G. Margaritondo, M. Onellion, *ibid.* **71**, 4051 (1993).
5. D. S. Dessau *et al.*, *ibid.* **66**, 2160 (1991).
6. B. L. Blackford, *Physica* **55**, 475 (1971), particularly figure 4; *Phys. Rev. B* **5**, 1171 (1972); _____ and R. H. March, *Phys. Rev.* **186**, 397 (1969).
7. Y. Chang *et al.*, *Phys. Rev. B* **39**, 4740 (1989).
8. A. V. Chubukov and S. Sachdev, *Phys. Rev. Lett.* **71**, 169 (1993).
9. P. Monthoux and D. Pines, *Phys. Rev. B* **49**, 4261 (1994), and references therein.
10. R. J. Kelley *et al.*, in preparation.
11. G. D. Mahan, *Phys. Rev. Lett.* **71**, 4277 (1993), and references therein.
12. A. A. Abrikosov, *Physica C* **214**, 107 (1993).
13. S. Chakravarty, A. Sudbø, P. W. Anderson, S. Strong, *Science* **261**, 337 (1993).
14. J. F. Annett, *Adv. Phys.* **39**, 83 (1990).
15. J. Betouras and R. Joynt, unpublished material.
16. The idea of a two-component order parameter has been applied for heavy fermion systems. See, for example, R. Joynt, *Phys. Rev. Lett.* **71**, 3015 (1993), and references therein.
17. We thank D. Lynch, C. Olson, and R. Liu, who made their computer code on the superconducting gap available for us. C. Olson kindly showed us his heater design. We benefited from H. Ding's and R. Liu's advice about improving electron energy analyzer resolution. M. Winokur kindly showed us the use of GNUPLOT graphics. A. Umezawa supervised our ac susceptibility measurements. We benefited from conversations with R. Schrieffer, J. Annett, A. Chubukov, R. Klemm, R. Dynes, N. Goldenfeld, A. Gurevich, K. Johnson, R. Joynt, D. Pavuna, and D. Tanner. The staff of the Wisconsin Synchrotron Radiation Center (SRC), particularly R. Pedley, was most helpful. Financial support was provided by the U.S. National Science Foundation, both directly (DMR-9214707) and through support of the SRC (DMR-9212658) by Ecole Polytechnique Fédérale Lausanne and the Fonds National Suisse de la Recherche Scientifique, and by Deutsche Forschungsgemeinschaft.

8 September 1994; accepted 1 December 1994

A Neutral Templating Route to Mesoporous Molecular Sieves

Peter T. Tanev and Thomas J. Pinnavaia*

A neutral templating route for preparing mesoporous molecular sieves is demonstrated based on hydrogen-bonding interactions and self-assembly between neutral primary amine micelles (S°) and neutral inorganic precursors (I°). The S° I° templating pathway produces ordered mesoporous materials with thicker framework walls, smaller x-ray scattering domain sizes, and substantially improved textural mesoporosities in comparison with M41S materials templated by quaternary ammonium cations of equivalent chain length. This synthetic strategy also allows for the facile, environmentally benign recovery of the cost-intensive template by simple solvent extraction methods. The S° I° templating route provides for the synthesis of other oxide mesostructures (such as aluminas) that may be less readily accessible by electrostatic templating pathways.

Mobil Oil Corporation researchers discovered the M41S family of mesoporous molecular sieves from a self-assembly process involving electrostatic interactions between positively charged quaternary ammonium micelles and inorganic anions as framework precursors (*1*). Recently, Schüth, Stucky, and their co-workers (*2*) extended the electrostatic assembly approach by proposing four complementary synthesis pathways.

Pathway 1 involved the direct cocondensation of a cationic surfactant (S^+) with anionic inorganic species (I^-) to produce assembled ion pairs (S^+ I^-). The original synthesis of MCM-41 silicates is a prime example of this pathway (*1*). In the charge-reversed situation (pathway 2), an anionic template (S^-) was used to direct the self-assembly of cationic inorganic species (I^+) through S^- I^+ ion pairs. Pathways 3 and 4 involved counterion (X^- or M^+)–mediated assemblies of surfactants and inorganic species of similar charge. These counterion-mediated pathways produced assembled solution species of the type S^+ X^- I^+ (where X^- = Cl^- or Br^-) or S^- M^+ I^- (where M^+ = Na^+ or K^+), respectively. The viability of pathway 3 was demonstrated by the synthesis of a hexagonal MCM-41 silica with quaternary ammonium cations under strongly acidic conditions (5 to 10 M HCl or HBr) to generate and assemble positively charged framework precursors (*2*). Also, we have reported (*3*) the preparation of a mesoporous silica molecular sieve and a Ti-substituted analog by the acid-catalyzed hydrolysis of inorganic alkoxide precursors in the presence of primary ammonium ions.

Department of Chemistry and Center for Fundamental Materials Research, Michigan State University, East Lansing, MI 48824, USA.

*To whom correspondence should be addressed.

Because all of the above pathways are based on charge matching between ionic surfactants and ionic inorganic reagents, the template is strongly bonded to the charged framework and difficult to recover. In the original Mobil approach (*1*), the template was not recovered but simply burned off by calcination at elevated temperatures. Recently, it has been demonstrated that the ionic surfactant in pathway 1 materials can be removed by ion-exchange in cation donor solutions (*4*). Also, the template-halide ion pairs in the framework of acidic pathway 3 materials are displaced by ethanol extraction (*2*). Thus, ionic template recovery is possible, provided that exchange ions or ion pairs are present in the extraction process.

Here we report a neutral templating route to mesoporous molecular sieves that is complementary to pathways 1 through 4. Our approach is based on hydrogen bonding and self-assembly between neutral primary amine micelles (S°) and neutral inorganic precursors (I°). This neutral S° I° templating route, which we denote pathway 5, produces mesostructures with larger wall thicknesses, small scattering domain sizes, and complementary textural mesoporosities relative to materials produced by pathways 1 and 3. The thicker pore walls improve the thermal and hydrothermal stability (*5*) of the mesopore framework, and the small crystallite domain size introduces textural mesoporosity, which facilitates accessing the framework-confined pores (*3*, *6*). The S° I° pathway also allows for the facile recovery of the template by simple solvent extraction.

We have prepared ordered mesoporous materials in the presence of C_8 to C_{18} primary amines in water with ethanol as a cosolvent. The use of a cosolvent improved template solubility. The synthesis of a hexagonal mesoporous silica with dodecyl amine (DDA) as the template illustrates the novelty of our synthetic strategy. In a typical preparation, tetraethyl orthosilicate (1.0 mol) was added under vigorous stirring to a solution of amine (0.27 mol) in ethanol (9.09 mol) and deionized water (29.6 mol). The reaction mixture was aged at ambient temperature for 18 hours, and the resulting hexagonal mesoporous silica (HMS) was air-dried on a glass plate. We removed the template by mixing 1 g of the air-dried HMS with 150 ml of hot ethanol for 1 hour. The product was then filtered and washed with a second 100-ml portion of ethanol. This extraction procedure was repeated twice, and the crystalline product (denoted HMS-EE) was air-dried at 353 K.

The powder x-ray diffraction (XRD) patterns of HMS and HMS-EE are shown in Fig. 1. Included for comparison is the pattern for an HMS sample calcined in air at 903 K for 4 hours (designated HMS-C). All patterns are similar and exhibit a single diffraction peak corresponding to *d* spacing of 3.8, 4.0, and 3.5 nm, respectively. Higher order Bragg reflections of the hexagonal structure are not resolved. However, we and others have demonstrated (*3*, *7*) that similar "single-reflection" MCM-41–type products still have short-range hexagonal symmetry. The diffuse scattering at ~5° is attributable to *hk*0 reflections that are broadened as a result of small crystallite domain effects. We believe that strong electrostatic interactions and charge matching are essential for the formation of the long-range–ordered hexagonal phase. The single XRD reflections and small x-ray scattering domain sizes of our hexagonal materials suggest that their formation is governed by weak, nonionic interactions. We note that the intensity of the d_{100} reflection of HMS-C is twice, and that of HMS-EE four times that of the as-synthesized HMS. Thus, the removal of the template by solvent extraction tends to preserve the crystallinity of the product, whereas local heating during calcination might cause some degradation of the mesoporous framework.

Important trends are revealed by a comparison in Fig. 2 of the N_2 adsorption-desorption isotherms and the corresponding Horvath-Kawazoe (*8*) pore size distribution curves for HMS-C and HMS-EE. Both samples exhibit complementary textural and framework-confined mesoporosity, as evidenced by the presence of two separate, well-expressed hysteresis loops. The isotherm for HMS-EE is similar to that for HMS-C. The specific surface areas of both samples are also similar (1000 and 1150 m^2/g, respectively). These results imply that the template is efficiently removed by solvent extraction from the pore network of our molecular sieve. The ethanol-extracted product is thermally stable, as evidenced by the retention of the 4.1-nm *d* spacing after calcination in air at 723 K for 7 hours. In accord with the properties of MCM-41 materials, both samples exhibit a hysteresis loop in the P_i/P_o = 0.15 to 0.4 region (*9*) indicative of framework-confined mesopores (Fig. 2). The size of these pores, as determined from the pore size distribution curves (see Fig. 2 insert), is 2.4 and 2.7 nm for HMS-C and HMS-EE, respectively. The smaller pore size of HMS-C could be attributed to the partial collapse of the mesoporous framework on calcination.

The properties of the calcined mesoporous silicas obtained by the S° I° and the electrostatic templating routes are summarized in Table 1. The following features are evident: (i) All mesoporous products templated with neutral amines of C_8 to C_{18} alkyl chain length exhibit single XRD reflections with d_{100} and a_o values that are larger than those of the corresponding MCM-41 samples prepared with ionic surfactants. (ii) The scattering domain sizes of the materials prepared by neutral templating are much smaller (≤17 nm) than those of the corresponding MCM-41 materials (≥93 nm). (iii) The HK framework-confined mesopore sizes are similar for both classes of materials prepared with surfactants of equivalent alkyl chain length. (iv) The framework wall thicknesses of our S° I° mesostructures (≥1.7 nm) are consistently larger than those of MCM-41 materials prepared from charged templates of equivalent

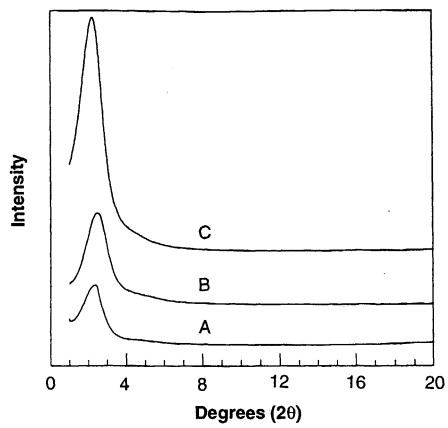

Fig. 1. Powder XRD patterns of (**A**) HMS, (**B**) HMS-C, and (**C**) HMS-EE. The patterns were measured on a Rigaku Rotaflex diffractometer equipped with a rotating anode and Cu-K_α radiation (λ = 0.15418 nm).

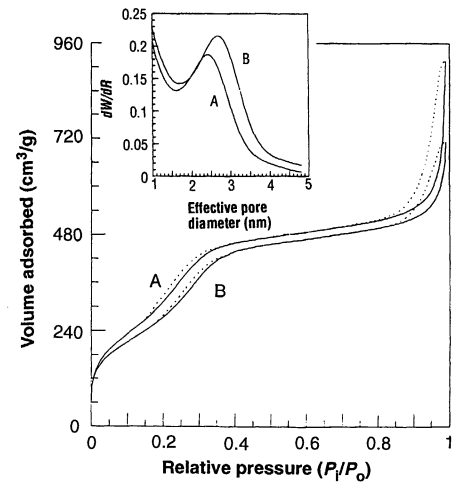

Fig. 2. Nitrogen adsorption (—) and desorption (- -) isotherms for (**A**) HMS-C and (**B**) HMS–EE (*9*). (**Insert**) The corresponding Horvath-Kawazoe pore size distribution curves; *dW/dR* is the derivative of the normalized nitrogen volume adsorbed with respect to the pore diameter of the adsorbent. Before measurement, samples were evacuated overnight at 423 K and 10^{-6} torr. The isotherms were measured at 77 K on a Coulter Omnisorp 360CX Sorptometer with a continuous adsorption procedure.

alkyl chain length. The much thicker framework walls, together with the small scattering domain size and substantial textural mesoporosity of our materials, provide strong evidence in support of the weak templating forces governing the S° I° self-assembly mechanism. The ability to completely displace the template from the mesoporous framework by ethanol extraction, without the need for exchange ions or ion pairs, also supports the neutral templating mechanism. The efficient removal of the template was confirmed by the absence of C–H vibrations in the infrared spectrum of the ethanol-extracted product and by the absence of a TGA weight loss over the temperature range where the amine normally undergoes thermal decomposition (*10*).

Further evidence in support of the postulated mechanism was obtained by ^{14}N nuclear magnetic resonance (NMR) spectroscopy of neutral and intentionally protonated primary amine template solutions and a wet HMS product (*11*). In agreement with the reported ^{14}N NMR spectra of aqueous cetyltrimethylammonium cation solutions (*12*), the spectrum of a partially protonated DDA solution (0.27 DDA : 0.054 HCL : 9.09 C_2H_5OH : 29.6 H_2O) exhibits a single isotropic resonance due to the ^{14}N nucleus in a tetrahedral environment (one-fifth of the DDA protonated). This implies that significant concentrations of protonated amine should readily be detected by the applied NMR technique. In the absence of tetrahedral symmetry, the signal produced by the ^{14}N nucleus is broad and cannot be detected (*12*). Because the ^{14}N NMR spectrum of our neutral DDA templating solution is featureless, the fraction of nitrogen centers adopting a tetrahedral environment is insignificant. In addition, the ^{14}N NMR spectrum of the wet HMS product also lacks the isotropic resonance of a protonated amine. This result further verifies that the templating of our ordered mesoporous materials occurs primarily by the assembly of neutral amine molecules.

We propose that the formation of our silica mesostructures occurs through the organization of the surfactant molecules into neutral rodlike micelles. On hydrolysis of tetraethyl orthosilicate, the resultant $Si(OC_2H_5)_{4-x}(OH)_x$ species most likely participate in hydrogen-bonding interactions with the surfactant head groups. Further hydrolysis and condensation of the silanol groups results in short-range hexagonal packing of the micelles and framework wall formation. The versatility of this neutral templating approach is confirmed by our preparation of a nonlayered templated alumina and a Ti-substituted analog. These ordered materials are obtained by a procedure similar to that for HMS with neutral octyl or dodecyl amine as the template and neutral aluminum and titanium-aluminum alkoxide precursors. Both products exhibit strong d_{100} reflections, accompanied with more or less pronounced diffuse scattering centered at diffraction angles where the remaining *hk*0 reflections of the hexagonal phase are expected. In addition, we have prepared a templated lamellar SiO_2 with neutral 1,12-diaminododecane. This product did not collapse on removal of the template by calcination in air at 903 K for 4 hours.

The neutral S° I° templating route to regular mesoporous materials offers distinct advantages over the electrostatic templating methods of pathways 1 to 4. The ordered mesostructures obtained by our templating strategy have larger framework wall thicknesses, small crystallite domain sizes, and complementary textural mesoporosities in comparison with M41S materials templated by quaternary ammonium cations of equivalent chain length. In addition, the use of a nonionic templating approach allows for the environmentally benign recovery of the cost-intensive template by simple solvent extraction. This circumvents the need for exchange ions or ion pairs to displace the ionic template. The neutral S° I° route complements electrostatic templating pathways to mesostructured materials and could facilitate the synthesis of ordered compositions (such as aluminas) that may be less readily accessible by ionic templating.

Table 1. Properties of calcined mesoporous silicas assembled by different templating routes. The scattering domain size was determined from the line width of the d_{100} x-ray reflection. The repeat distance (a_o) between pore centers of the hexagonal structure is calculated from the XRD data with the formula $a_o = 2d_{100}/\sqrt{3}$. The framework-confined mesopore size (HK pore size) was determined by Horvath-Kawazoe (HK) analysis (*8*) of the N_2 adsorption isotherms. The framework wall thickness is determined by subtracting the HK mesopore size from the repeat distance between pore centers. Dashes indicate that the variable was not measured.

Templating route	Template alkyl chain length	d_{100} (nm)	Scattering domain size (nm)	a_o (nm)	HK pore size (nm)	Wall thickness (nm)
S° I°	C_8	3.6	11.0	4.2	1.6	2.6
S° I°	C_{10}	3.4	15.7	3.9	2.0	1.9
S° I°	C_{12}	3.6	17.0	4.2	2.4	1.8
S° I°	C_{14}	3.7	15.4	4.3	2.2	2.1
S° I°	C_{16}	4.8	11.4	5.5	2.5	3.0
S° I°	C_{18}	4.2	14.5	4.8	3.1	1.7
$S^+ I^-$	C_8*	2.7	–	3.1	1.8	1.3
$S^+ I^-$	C_{10}*	2.9	–	3.3	2.2	1.1
$S^+ I^-$	C_{12}†	3.1	240.3§	3.6	2.5	1.1
$S^+ I^-$	C_{14}*	3.3	–	3.8	3.0	0.8
$S^+ X^- I^+$	C_{16}	3.3	93.6	3.8	2.6	1.2
$S^+ I^-$	C_{16}‡	3.6	93.3§	4.2	3.0	1.2
$S^+ X^- I^+$	C_{18}	3.4	137.6	3.9	2.7	1.2

*From (*1*). †From (*13*). ‡From (*14*). §Calculated from the published XRD patterns.

REFERENCES AND NOTES

1. C. T. Kresge, M. E. Leonowicz, W. J. Roth, J. C. Vartuli, J. S. Beck, *Nature* **359**, 710 (1992); J. S. Beck *et al.*, *J. Am. Chem. Soc.* **114**, 10834 (1992).
2. Q. Huo *et al.*, *Nature* **368**, 317 (1994).
3. P. T. Tanev, M. Chibwe, T. J. Pinnavaia, *ibid.*, p. 321.
4. D. D. Whitehurst, U.S. Patent 5,143,879 (1992).
5. S. B. McCullen and J. C. Vartuli, U.S. Patent 5,156,829 (1992); N. Coustel, F. Di Renzo, F. Fajula, *J. Chem. Soc. Chem. Commun.* **1994**, 967 (1994).
6. N. S. Gnepr *et al.*, *C. R. Acad. Sci. Ser. 2* **309**, 1743 (1989); B. Chauvin, F. Fajula, F. Figueras, C. Gueguen, J. Bousquet, *J. Catal.* **111**, 94 (1988).
7. J. C. Beck *et al.*, World Organization patent 91/113090 (1991); R. Schmidt, D. Akporiaye, M. Stöcker, O. H. Ellestad, in *Zeolites and Related Microporous Materials, State of the Art 1994, Studies in Surface Science and Catalysis*, J. Weitkamp, H. G. Karge, H. Pfeifer, W. Hölderich, Eds. (Elsevier Science B. V., Amsterdam, 1994), vol. 84, pp. 61–68.
8. G. Horvath and K. J. Kawazoe, *J. Chem. Eng. Jpn.* **16**, 470 (1983).
9. P_i is the equilibrium pressure of the adsorbate, and P_o is the saturation pressure of the adsorbate at the temperature of the adsorbent; the adsorbed volume is at standard temperature and pressure.
10. The thermogravimetric analysis (TGA) was performed on a Cahn system TG analyzer with a heating rate of 5 K/min. The analysis of the as-synthesized HMS revealed ~47% total weight loss on heating to 1073 K. Three distinguishing endothermic features centered at approximately 421, 511, and 733 K were observed. The first effect is attributed to the release of adsorbed water, the second to the desorption and decomposition of the template, and the third to dehydroxylation of the surface. In contrast, the TGA of HMS-EE gave 11% total weight loss with ~9% corresponding to water desorption and surface dehydroxylation.
11. The ^{14}N NMR spectra were recorded at 28.88 MHz on a Varian 400 VXR solid state spectrometer. Chemical shifts were referenced to an aqueous ammonium chloride solution. A quadrupole echo sequence with quadrature phase cycling was used with a 90° pulse length of 4 μs and an interpulse delay (τ) of 115 to 120 μs. Depending on the sample, 30 to 20,000 transients were collected with a spectral width of 200 kHz and a recycle time of 140 ms.
12. C.-Y. Chen, H.-X. Li, M. E. Davis, *Microporous Mater.* **2**, 27 (1993).
13. K. M. Reddy, I. Moudrakovski, A. Sayari, *J. Chem. Soc. Chem. Commun.* **1994**, 1059 (1994).
14. C.-Y. Chen, H.-X. Li, M. E. Davis, *Microporous Mater.* **2**, 17 (1993).

15. The partial support of this research by NSF through grant CHE-9224102 is gratefully acknowledged. We thank K. M. Johnson for technical assistance in obtaining the NMR results.

25 August 1994; accepted 10 November 1994